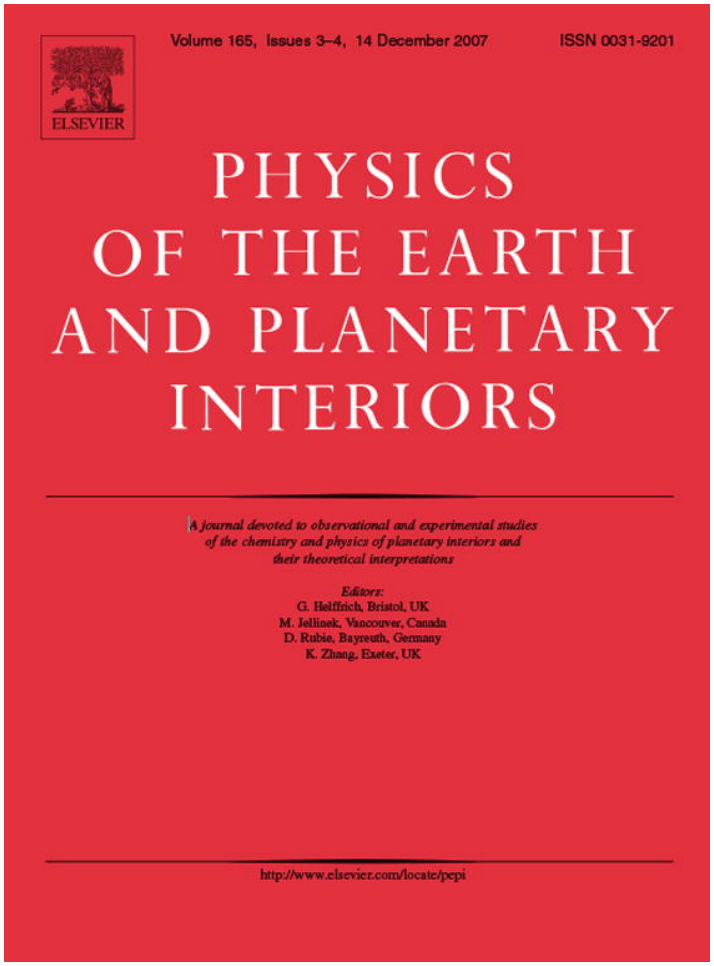

Available online at www.sciencedirect.com
ScienceDirect
Physics of the Earth and Planetary Interiors 165 (2007) 158–175
PHYSICS OF THE EARTH AND PLANETARY INTERIORS
www.elsevier.com/locate/pepi

Analysis of relaxation temporal patterns in Greece through the RETAS model approach

Gospodinov Dragomir [a], Karakostas Vassilios [b], Papadimitriou Eleftheria [b,*], Ranguelov Boyko [a]

[a] *Geophysical Institute of the Bulgarian Academy of Science, Bulgaria*
[b] *Geophysics Department, Aristotle University of Thessaloniki, GR54124 Thessaloniki, Greece*

Received 21 June 2007; received in revised form 30 August 2007; accepted 5 September 2007

Abstract

The temporal decay of eight aftershock sequences in the area of Greece after 1975 was examined with main shocks magnitudes of $M_w \geq 6.6$. The analysis was done through the restricted epidemic type aftershock sequence (RETAS) stochastic model, which enables the possibility to recognize the prevailing clustering pattern of the relaxation process in the examined areas. In four of the cases the analysis selected the epidemic type aftershock sequence (ETAS) model to offer the most appropriate depiction of the aftershock temporal distribution which presumes that all shocks to the smallest ones in the sample can cause secondary aftershocks, while for the rest of the sequences triggering potential seems to have aftershocks above a certain magnitude threshold (RETAS model) and they are expected to induce secondary activity.

The models, developed on aftershock data, were also applied to forecast real seismicity after the conclusion of the aftershock sequences. For four out of eight cases, we obtained promising estimations of ensuing seismicity after the end of the sequences with models based only on aftershock data. Some features of the RETAS model simulation were also studied, like simulating magnitudes, revealing that it is reasonable to consider in the model the temporal behavior of the aftershocks' magnitudes as well. Stochastic modeling was also applied to estimate the duration of the relaxation process, assuming that the end of each sequence is marked by the divergence of real seismicity from the modified Omori formula (MOF) model, the latter known to represent pure aftershock activity. The obtained results give an indication that possibly low stressing rate results in longer duration of the relaxation process in a region.

Keywords: Aftershock sequence; Stochastic models; RETAS; ETAS; Relaxation process; Simulation

1. Introduction

Stochastic modeling has become a major tool in examining the clustering properties of earthquake occurrences. Former tendency of carrying out declustering algorithms that remove aftershocks from a catalog is now replaced by the application of a number of stochastic processes to fit the clustering behavior of a sequence. This allows making use of all available information in a seismic catalog and thus aftershock data can in many cases help in the detection of anomalous seismicity changes like quiescence or activation prior to a large earthquake (Matsu'ura, 1986; Zhao et al., 1989; Ogata et al., 2003; Ogata, 2005a,b; Drakatos, 2000). The great interest

* Corresponding author. Tel.: +30 2310 998488; fax: +30 2310 998528.
E-mail addresses: drago_pld@yahoo.com (D. Gospodinov), vkarak@geo.auth.gr (V. Karakostas), ritsa@geo.auth.gr (E. Papadimitriou), branguelov@gmail.com (B. Ranguelov).

0031-9201/$ – see front matter © 2007 Elsevier B.V. All rights reserved.
doi:10.1016/j.pepi.2007.09.001

dedicated by many researchers of the aftershock activity to statistical methods is obviously linked to the vast possibilities, which they offer in studying and modeling the relaxation process. Among them, the most important are development of detailed temporal patterns, elaboration of adequate stochastic models of aftershock occurrences, detection of anomalous seismicity changes before strong aftershocks or before forthcoming main shocks, providing stochastic grounds for seismic hazard analysis etc.

One can find a number of point processes in the literature that concern aftershock clusters in time or both in space and time (Ogata, 1988, 1993, 1998; Kagan, 1991; Vere-Jones, 1992; Musmeci and Vere-Jones, 1992; Rathbun, 1993, 1994; Schoenberg, 1997; Console and Murru, 2001; Zhuang et al., 2002; Ogata et al., 2003; Console et al., 2003; Gospodinov and Rotondi, 2006). One of the first approaches to model the gradual decay of the aftershocks triggered by a strong earthquake is the so-called Omori law (Omori, 1894). Utsu (1970) transformed it into the modified Omori formula (MOF), which is most widely used up to now. It is grounded on the basic assumption that all the events in an aftershock sequence are triggered by the stress field change due to the main shock, follow a nonstationary Poisson process and there is no subclustering in the sequence. When we deal with more complex cases and especially when smaller aftershocks are considered, temporal clustering becomes apparent. Under such circumstances and particularly when we study some conspicuous secondary aftershock activities of large aftershocks, the single modified Omori formula cannot provide the best prediction of the rate decay as demonstrated in Guo and Ogata (1997).

These cascading complex features of aftershocks motivated Ogata (1988) to formulate the epidemic type aftershock sequence (ETAS) model, based on the idea of self-similarity and extending the capacity of generating secondary events to every aftershock of the sequence. The two models constitute limit cases, the MOF model with only one parent-event and the ETAS model in which every event shares in the generation of the subsequent ones. The vast variability of different geotectonic conditions and different temporal patterns of aftershock occurrences requires some intermediate cases to be considered and there is a range of triggering models, which stand between the MOF and ETAS (Vere-Jones, 1970; Vere-Jones and Davies, 1966; Ogata, 2001; Gospodinov and Rotondi, 2006). In their work on the restricted epidemic type aftershock sequence (RETAS) model Gospodinov and Rotondi (2006) examined a case in which, as in Ogata (2001), triggering capabilities possess events with magnitudes larger than or equal to a threshold, M_{th}. The RETAS model is similar to the ETAS one, but leaving a gap between the magnitude M_{th} of the triggering event and the magnitude cut-off M_0. The idea is borrowed by Bath's law (Bath, 1965, 1973), which affirms certain difference between main shock's magnitude and the one of the largest aftershock. By varying M_{th} one can examine all RETAS models between the MOF and the ETAS model on the basis of the Akaike Information Criterion (AIC; Akaike, 1974).

The purpose of this paper is to study stochastic features of the relaxation process after some strong earthquakes in Greece by the RETAS model approach. There are a number of papers which analyze aftershock occurrences in that area on the basis of the MOF model (Latoussakis et al., 1991; Drakatos and Latoussakis, 1996; Drakatos, 2000) but in our work we want to make use of the enhanced capacities of the RETAS model to identify the most adequate stochastic patterns of time clustering for the data. The model has the advantage to verify all its versions between the MOF and the ETAS model including them as limit cases. Our aim is also to test how well an aftershock occurrence model can forecast the seismicity rate after the sequence is over, examine some aspects of the RETAS model simulation and analyze its applicability to assess the relaxation duration. We expect to shed more light on whether different seismotectonic regimes may reflect in stochastic dissimilarity.

2. RETAS model formulation

Each stochastic model is developed after some basic physical assumptions. For the MOF it is regarded that the total relaxation process is controlled by the stress field changes caused by the main shock. The aftershocks are conditionally independent and follow a nonstationary Poisson process. The ETAS model (Ogata, 1988) assumes that every aftershock in a certain zone can trigger further shocks and the contribution of any previous earthquake to the occurrence rate density λ_j of the subsequent events can be decomposed into separate terms representing the time and magnitude distribution as

$$\lambda_j(t, m) = h(t - t_j | m_j) = k(m_j)g(t - t_j) \quad (1)$$

Here $h(t - t_j | m_j)$ is the functional form of the rate density after the jth event, which depends on the elapsed time after this shock and on its magnitude. As Ogata (1988) suggested, this function is decomposable and the temporal decay rate follows the MOF $g(t) \propto (t+c)^{-p}$ while the functional form of $k(m_j)$ is chosen to be exponential on the basis of the linear correlation between the logarithm of the aftershock area and the main shock's magnitude, studied extensively by Utsu and Seki (1955). Hence, the

expected resultant rate density of aftershocks is given by Ogata (1988):

$$\lambda(t|H_t) = \mu + \sum_{t_j<t} \frac{K_0\, e^{\alpha(m_j - M_0)}}{(t - t_j + c)^p} \quad (2)$$

where μ (shocks/day) is the rate of background activity, the history H_t consists of the times t_j (days) and magnitudes m_j of all the events which occurred before t and the summation is taken over every jth aftershock with a magnitude stronger than the cut-off $m_j \geq M_0$ i.e. over all events in the sample. The main shock in this case is indicated by $j = 1$. In probabilistic terminology, the first term on the right-hand side of (2) stands for the "independent" seismicity and the "induced" seismicity is represented by a superposition of the modified Omori functions shifted in time. In formula (2) the coefficient α measures the magnitude efficiency of a shock in generating its aftershock activity and K_0 (shocks/day) measures the productivity of the aftershock activity during a short period right after the mainshock (cf. Utsu, 1970; Reasenberg and Jones, 1994). Like in the MOF (Utsu, 1970) p is a coefficient of attenuation, which changes in value usually from 0.9 to 1.5, regardless of the cutoff magnitude. The variability in p-value may reflect variations in the structural heterogeneity, stress and temperature in the crust (Kisslinger and Jones, 1991; Utsu et al., 1995), but it is not yet clear which of these factors is most significant in controlling the p-value. The parameter c in formula (2) is a regularizing time scale that ensures that the seismicity rate remains finite close to the mainshock.

The MOF and the ETAS model are two limit cases, the former with only one parent-event and the latter with all events sharing in the generation of the subsequent ones. Gospodinov and Rotondi (2006) offer the restricted epidemic type aftershock sequence (RETAS) model, which is based on the assumption that not all events in a sample but only aftershocks with magnitudes larger than or equal to a threshold M_{th} can induce secondary seismicity. Then the conditional intensity function for the model is formulated as

$$\lambda(t|H_t) = \mu + \sum_{\substack{t_j < t \\ m_j \geq M_{th}}} \frac{K_0\, e^{\alpha(m_j - M_0)}}{(t - t_j + c)^p} \quad (3)$$

Following the Bath's law in seismology there should be a gap between the magnitudes of the main shock and the strongest aftershock. Introducing this rule to be valid for all secondary sequences in the data would mean that a gap could also be expected between the triggering level M_{th} and the magnitude cut-off M_0. An advantage of the RETAS model is that this gap is not fixed and by varying M_{th} all RETAS versions between the MOF and the ETAS model can be examined on the basis of the Akaike criterion given by

$$\text{AIC} = -2 \max \log L(\theta) + 2k \quad (4)$$

where θ stands for the model parameters, k the number of parameters of the model and $\log L$ is the logarithm of the likelihood function, given by

$$\log L(\theta) = \sum_{i=1}^{N} \log \lambda_\theta(t_i|H_{t_i}) - \int_0^T \lambda_\theta(t|H_t)\, dt \quad (5)$$

In the above formula N is the number of considered aftershocks and T is the time period which they cover.

By allowing the triggering magnitude M_{th} to vary from the cut-off magnitude M_0 to the main event magnitude, we consider a number of RETAS models and for each of them we calculate the AIC criterion value through formula (4). The smallest value of the Akaike criterion recognizes the best-fit model (Akaike, 1974). Gospodinov and Rotondi (2006) have developed a program in Fortran 95 which exploits subroutines of the IMSL library to maximize the likelihood of the RETAS model following a quasi-Newton method and we apply the same software in this study.

To identify possible discrepancies between the best-fit model and the data we apply an approach offered by Ogata (1988). He uses the residual analysis to evaluate the goodness of fit after choosing the best-fit model. The integration of the nonnegative conditional intensity function produces a transformation of time from t to $\tau = \Lambda(t)$ so that the occurrence times t_j are transformed 1:1 into τ_j and the earthquakes follow the standard stationary Poisson process on the new axis if the intensity function is the true one for the data:

$$\tau = \Lambda(t) = \int_0^t \lambda(s)\, ds \quad (6)$$

The process is called a residual process and its mean and standard deviation are used to study possible deviations of the data from the model (Ogata, 1992).

3. Seismotectonic regime of the study area and data

Various researchers have presented much information on basic problems regarding active tectonics and deformation in the broader Aegean area (Fig. 1). It is one of the most active tectonic regions of the Alpine–Himalayan belt, with its most prominent tectonic feature the sub-

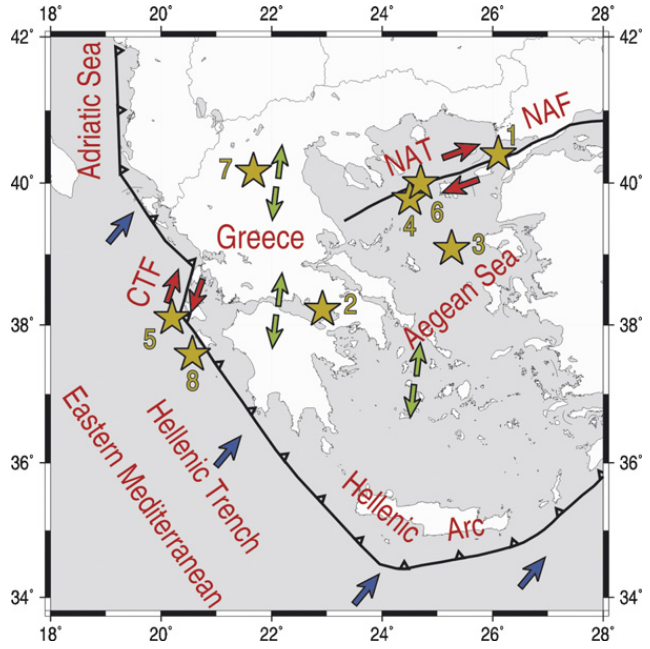

Fig. 1. Main geodynamic characteristics of the broader Aegean region (NAF: North Anatolian Fault; NAT: North Aegean Trough; CTF: Cephalonia Transform Fault). Arrows indicate the relative plate motion (convergence along the Hellenic Arc and the collision zone, strike slip faulting in CTF and North Aegean, and extension in the back arc Aegean area). The epicenters of the main shocks of the studied sequences studied are depicted as stars, and the numbers next to its epicenter denote the event number in chronological order of occurrence. (For interpretation of the references to colour in this figure legend, the reader is referred to the web version of the article.)

duction of the eastern Mediterranean lithosphere under the Aegean Sea along the Hellenic Arc (Papazachos and Comninakis, 1970, 1971). The seismicity is very high throughout the arc, which is dominated by thrust faulting with a NE–SW direction of the axis of maximum compression. A belt of thrust faulting runs along the eastern Adriatic shore, continues south along the coastal regions of Albania and northwestern Greece and terminates at central Ionian Islands. This type of faulting is connected with the continental collision between Outer Hellenides and the Adriatic microplate. The direction of the maximum compression axis is almost normal to the direction of the Adriatico-Ionian geological zone. Between continental collision to the north and oceanic subduction to the south, in the area of central Ionian Islands, the dextral strike-slip Cephalonia Transform Fault (CTF) is observed (Scordilis et al., 1985), in agreement with the known relative motion of the Aegean and eastern Mediterranean. The back-arc area, south Aegean Sea and continental Greece is dominated by extension. North Aegean Sea is characterized by a combination of right-lateral shear and extension. McKenzie (1970, 1972, 1978) showed that the northward motion of the Arabian plate pushes the smaller Anatolian plate westwards along the North Anatolian fault, continuing along the North Aegean Trough (NAT) region, which is the boundary between the Eurasian and south Aegean plates. Right-lateral strike-slip motion associated with the North Anatolian Fault (NAF) appears to become more distributed in the northern Aegean Sea. This motion is transferred into the Aegean but in a south-westerly direction. This style of faulting is consistent with several fault plane solutions of recent strong earthquakes (Papazachos et al., 1998a).

The study area has frequently experienced strong earthquakes accompanying with an intense aftershock activity. In our study, we selected to examine the seismic sequences with main shock magnitude $M \geq 6.6$. The threshold magnitude of 6.6 was chosen to satisfy both the needs of our model, since an adequate number of aftershocks above a certain minimum magnitude are needed for the analysis and this number increases proportionally with the main shock magnitude in general, and on the other hand to obtain a satisfactory number of aftershock sequences. Eight such cases are available and the main shocks epicenters are depicted as stars in Fig. 1 (see also Table 1). Phases from the International Seismological Center and local stations were used for the relocation of the earthquakes by applying modern location techniques. The magnitudes are taken from the earthquake catalog of Papazachos et al. (2006), expressed as equivalent moment magnitudes (Papazachos et al., 1997).

Four out of the eight seismic sequences took place in the North Aegean Sea (1975 in Saros gulf, 1981 in the central part of North Aegean Sea, and 1982 and 1983 along the North Aegean Trough). Dextral strike-slip faulting dominates the northern Aegean Sea area as the North Anatolian fault prolongates into the northern Aegean Sea, where it bifurcates into two main branches of NE–SW trend. Parallel secondary faults are also recognized from seismicity and fault plane solutions of recent strong earthquakes. This area has frequently experienced many destructive earthquakes some of them occurring very close in time, as indicated from both instrumental data and historical information. Two seismic sequences (1981 Alkyonides in Corinth gulf and 1995 Kozani in northern Greece) are associated with normal faulting that dominates in the back arc territory of Greece. Corinth gulf is an asymmetric half-graben, with the higher extension rates in continental Greece and frequent occurrence of strong ($M \geq 6.0$) earthquakes, although, the 1981 main shock was the largest one during the instrumental era. Kozani is an area of relatively low stressing rate in comparison with adjacent fault zones and the broader Greek territory in general, resulting in

Table 1
List of events with $M \geq 6.6$ that occurred in the territory of Greece during the last 30 years

Event number	Year	Date	Time UT	Latitude	Longitude	h (km)	M_w	Focal mechanism			Location	Reference
								Strike	Dip	Rake		
1	1975	27 March	05:15:08	40.400	26.100	13.0	6.6	68	55	−145	Saros	1
2	1981	24 February	20:53:37	38.220	22.920	5.3	6.7	264	42	−80	Alkyonides	1
3	1981	19 December	14:10:51	39.080	25.260	14.3	7.2	47	77	−167	North Aegean	2
4	1982	18 January	19:27:25	39.780	24.500	11.6	7.0	233	62	−177	North Aegean	1
5	1983	17 January	12:41:31	38.100	20.200	7.0	7.0	39	45	175	Kefalonia	3
6	1983	6 August	15:43:52	40.000	24.700	8.8	6.8	50	76	177	North Aegean	2
7	1995	13 May	08:47:47	40.160	21.670	14.0	6.6	252	41	−90	Kozani	4
8	1997	18 November	13:07:41	37.576	20.568	10.0	6.6	352	25	144	Zakynthos	5

(1) Taymaz et al. (1991); (2) Kiratzi et al. (1991); (3) Papadimitriou (1993); (4) Hatzfeld et al. (1997); (5) Louvari (2000).

very long recurrence times for strong events of this magnitude class. The central Ionian Islands, where the 1983 Kefalonia and 1997 Zakynthos seismic sequences took place, exhibit a high level of seismic activity. This is due to the fact that the Cephalonia Transform Fault, where the 1983 main shock took place, is the area with highest moment rate release in the whole Eurasia (Papazachos and Kiratzi, 1996). The 1997 Zakynthos earthquake is located at the northwestern edge of the Hellenic arc, thus associated with the subduction process, which results in high seismic activity.

4. Application of the RETAS model and results

Below we present the results obtained by the application of the RETAS stochastic model to analyze the relaxation process after the eight strong earthquakes, listed in Table 1.

4.1. Saros seismic sequence, 27 March 1975, $M_w = 6.6$

This earthquake occurred offshore west of the Sea of Marmara in the Gulf of Saros, a pull-apart basin associated with prolongation of the northern branch of the North Anatolian fault (NAF) into the Aegean Sea. The main shock focal mechanism indicates oblique dextral strike-slip rupture (Taymaz et al., 1991) with the fault plane striking at ENE–WSW consistent with the strike of the North Aegean Trough (NAT) at this site (Fig. 2a). We compile a catalog of aftershocks, up to the end of 1975, in a zone defined by the vertices 39.8°N, 25.4°E; 41.0°N, 26.8°E (Fig. 2a) and in a depth range up to $h = 20$ km, since it is well known that crustal seismicity in the Aegean region is confined to this depth range. The application of the ZMAP software package (Wiemer, 2001) for the recognition of the magnitude of completeness returns a value of $M_0 = 4.0$. For this magnitude cut-off only 29 events remain in the catalog and because of the small number of examined events the results for the Saros sequence should be considered with greater caution. In Fig. 3a, we plotted the obtained AIC values versus the triggering magnitude M_{th}. As it can be seen, the smallest AIC value for this sequence identifies the best-fit model to be RETAS with $M_{th} = 4.2$ and a background activity of $\mu = 0$ (Table 2). The relaxation pattern here is such that only events with magnitudes bigger or equal to 4.2 are supposed to cause secondary clustering.

The model-to-data fitness is verified graphically through the cumulative number curves. Substituting the maximum-likelihood (ML) estimates of the best model parameters in (3) we calculated the expected cumulative number curve and it is represented by a solid blue line in Fig. 4a, where the red circles indicate the real cumulative number of aftershocks. Fig. 4a depicts the process in real time while Fig. 4b the one for a transformed time axis after applying formula (6). Dashed lines stand for error bounds determined after the standard deviation of the model process. The bottom part (Fig. 4c) represents the residual process, from which it is easy to see that there is no significant discrepancy between model and real data, the real curve staying inside the error bounds.

The RETAS model was developed to describe not only aftershock activity, but also like ETAS (Ogata, 1998) it can be used to represent general seismic activity, too. Following this idea, we decided to test how well the model can 'predict' the seismic process in the same area after the examined time period. The model cumulative curve is calculated using the model parameter values obtained on the aftershock data sample only and the real aftershocks magnitudes (Table 2).

The results are illustrated in Fig. 4d–f and they expose that about 900 days after the main event the actual data diverges markedly from the model giving higher values

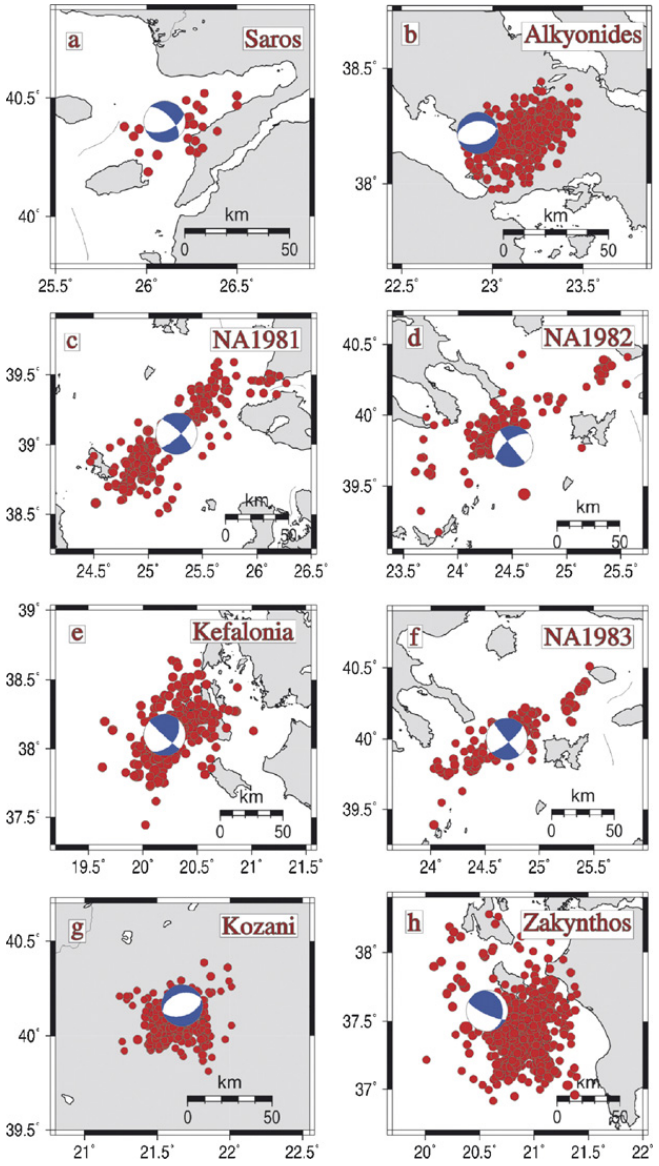

Fig. 2. Spatial distribution of the aftershocks (red dots) sequences. The main shocks fault plane solutions are depicted as lower hemisphere equal area projections. (a) Saros 1975; (b) Alkyonides 1981; (c) North Aegean 1981; (d) North Aegean 1982, (e) Kefalonia 1983; (f) North Aegean 1983; (g) Kozani 1995; (h) Zakynthos 1997. (For interpretation of the references to colour in this figure legend, the reader is referred to the web version of the article.)

for the cumulative number. We suppose parameter values might be underestimated because of some lack of events in the examined sample. In Fig. 4d, we also present the MOF model curve (green line) calculated after the ML estimates of the aftershock data. As the MOF model was designed to depict pure aftershock activity, we suggest that the deviation of real data from the model can be utilized to mark the duration of the relaxation process. For this sequence, the duration seems to be about 850 days after the main shock (indicated by an arrow in Fig. 4d).

4.2. Alkyonides seismic sequence, 24 February 1981; $M_w = 6.7$

An intense seismic sequence started on 24 February 1981 with a main shock of magnitude $M_w = 6.7$, whose epicenter was about 77 km to the W–NW of Athens. It is associated with normal faulting on an almost E–W striking and north dipping fault at the eastern part of the Corinth gulf. Strong aftershocks followed, one of them five hours later with a magnitude of $M_w = 6.4$ in a small distance of the main shock and one more in about 8 days later (4 March) with $M_w = 6.3$ associated with an antithetic fault. The relaxation process was examined in a polygon area with vertices 37.5N, 22.5E; 37.5N, 23.5E; 38.5N, 23.5E; 38.5N, 22.5E (Fig. 2b), inside which the crustal seismicity up to the end of 1981 is considered. The ZMAP software estimated the magnitude of completeness to be $M_0 = 3.7$ and we compiled 553 aftershocks stronger than this cut-off.

The aftershock sequence analysis distinguishes the RETAS model with a triggering magnitude of $M_w = 6.3$ to depict best the data (Fig. 3b and Table 2). The clustering type is such that the main shock, along with the two strong aftershocks, control events' temporal behavior. A more detailed inspection of Fig. 5b and c detects a relative quiescence period before the second strong aftershock (follow arrows). It starts the first day after the main shock and continues several days then turning to a relative rate increase one day before the $M_w = 6.3$. This is in concordance with the findings of other papers (Latoussakis et al., 1991; Papazachos et al., 1984).

The predicted cumulative curve of the best-fit model and the one of the MOF model calculated after the end of the studied period are presented in Fig. 5d (blue and green solid lines, respectively). Comparison with real data reveals that the latter follow the MOF line for quite a long time. In fact, if we use again the divergence between them to spot the end of the sequence it should have lasted not less than 2000 days (see arrow in Fig. 5d). This result is quite far from the ones obtained after a statistical study by Kourouzidis et al. (2004) for Greece but it does not seem so strange if we consider that the seismicity level after the aftershock sequence is not high. In regions of low seismicity an aftershock sequence can last much longer than the period, we estimated—for example for the Nobi earthquake ($M = 8.4$) of 1891 the aftershock duration was evaluated to be more than 100 years (Ogata, 1989).

As far as the best-fit RETAS model curve is concerned (blue line in Fig. 5d), it does not present a good forecast of real seismicity, which is quite expected as according to the model only earthquakes stronger than $M_w = 6.3$ can

Table 2
Maximum-likelihood estimates of the RETAS model parameters (best model is marked in gray)

Model	M_{th}	AIC	μ	K	α	c	p
Saros 1975; *M=6.6;* Mo=*4.0*							
RETAS (best)	4.3	59.151	0	0.023	1.638	0.020	1.094
	4.2	70.247	0.013	0.027	1.589	0.033	1.244
MOF	6.6	62.940	0	2.645	0.031	0.021	0.998
Alkyonides 1981; *M=6.7;* Mo=*3.7*							
RETAS (best)	6.3	-1965.67	0	28.186	0.00001	0.115	1.123
	6.3	-1955.88	0.044	29.006	0.00001	0.127	1.15
MOF	6.7	-1621.02	0	24.529	0.896	2.122	1.417
North Aegean 1981; *M=7.2;* Mo=*3.7*							
RETAS (best)	4.4	-376.068	0	0.043	1.759	0.051	1.023
	4.4	-373.84	0.111	0.047	1.778	0.104	1.175
MOF	7.2	-312.726	0	10.538	0.296	0.058	0.926
North Aegean 1982; *M=7.0;* Mo=*3.7*							
RETAS (best)	4.2	-119.535	0	0.046	1.713	0.037	1.049
	4.2	-118.156	0.099	0.035	1.887	0.108	1.313
MOF	7	-93.666	0	2.701	0.569	0.042	0.971
Kefalonia 1983; *M=7.0;* Mo=*4.2*							
ETAS (best)	4.2	-546.242	0	0.093	1.826	0.184	1.357
	4.2	-536.179	0.032	0.105	1.804	0.225	1.439
MOF	7	-219.203		8.736	0.687	0.809	0.996
North Aegean 1983; *M=6.8;* Mo=*3.8*							
ETAS (best)	3.8	-208.244	0	0.0181	2.270	0.071	1.145
	3.8	-199.134	0.037	0.018	2.271	0.094	1.224
MOF	6.8	-175.314	0	3.357	0.625	0.072	1.000
Kozani 1995; *M=6.6; Mo=3.5*							
ETAS (best)	3.5	-1868.87	0	0.067	1.572	0.056	1.291
	3.5	-1862.31	0.094	0.073	1.566	0.083	1.401
MOF	6.6	-1777.33	0	9.999	1.241	2.561	1.467
Zakynthos 1997; *M=6.6;* Mo=*3.8*							
ETAS (best)	3.8	-830.979	0	0.085	1.702	0.1406	1.192
	3.8	-821.982	0.064	0.093	1.683	0.171	1.251
MOF	6.6	-716.141	0	0.661	1.7119	0.812	0.907

induce secondary activity. Thus, in this case the model is adequate for an aftershock sequence, but not for normal seismicity.

4.3. North Aegean seismic sequence, 19 December 1981; $M_w = 7.2$

The main shock of this sequence occurred in the central part of North Aegean Sea. The focal mechanism (Taymaz et al., 1991; Kiratzi et al., 1991) indicates right-lateral strike-slip faulting striking northeast–southwest, parallel to the orientation of the NAT and in full agreement with the spatial distribution of the aftershocks (Fig. 2c). The strongest aftershock occurred eight days after the main shock having a magnitude of $M_w = 6.5$. We considered events with $M_w \geq 3.7$, above which the catalog was evaluated to be complete. A number of 297 aftershocks occurred in 1-year period in a region defined by the points 38.2°N, 24.8°E; 39.4°N, 26.4°E; 40.0°N, 25.8°E; 38.8°N, 24.25°E.

The clustering type recognized by the RETAS model analysis suggests that aftershocks with $M_{th} \geq 4.4$ are supposed to trigger secondary shocks (Fig. 3c). The best-fit RETAS model allows selection of some relative to model deviations of the data. At the end of the first day a 1-day activation starts, which was followed by a period of quiescence of about 4 days, after which a recovery of the process is observed 1 day before the strong $M_w = 6.5$ aftershock (consider arrows on Fig. 6c).

In Fig. 6d real data diverges (see arrow) from the MOF model (green line) about 870 days after the first shock occurrence and this is assumed to be a measure of the aftershock sequence duration. Real data departs also from the RETAS model (solid blue line) revealing that it does not supply a good guess of the seismic process after the end of the aftershock sequence.

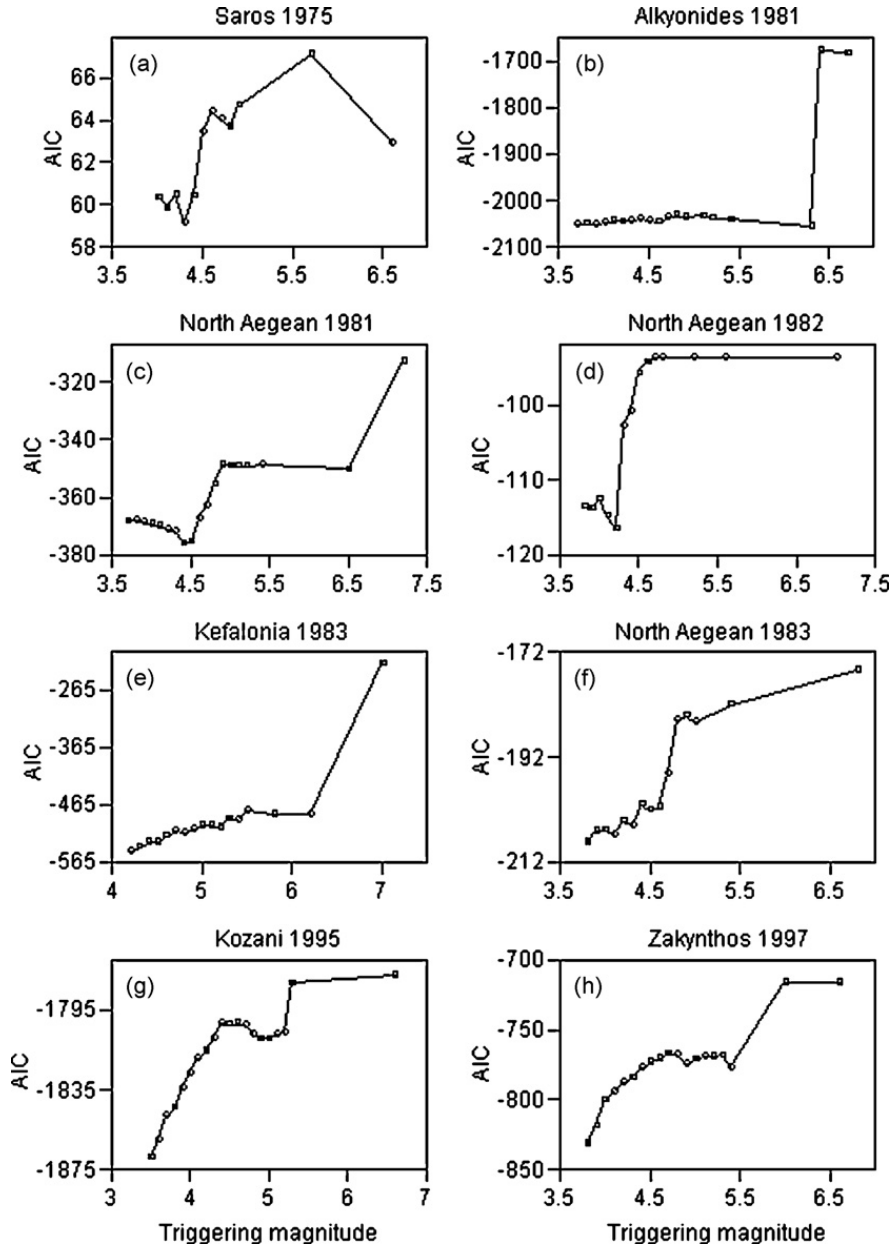

Fig. 3. Results from the RETAS model application – the Akaike Information Criterion (AIC) versus the triggering magnitude M_{th} for eight aftershock sequences in the area of Greece (see main events details in Table 1); (a) Saros 1975 – best-fit model is RETAS for $M_{th} = 4.3$; (b) Alkyonides 1981, best-fit model is RETAS for $M_{th} = 6.3$; (c) North Aegean 1981, best-fit model is RETAS for $M_{th} = 4.4$; (d) North Aegean 1982, best-fit model is RETAS for $M_{th} = 4.2$; (e) Kefalonia 1983, best-fit model is ETAS; (f) North Aegean 1983, best-fit model is ETAS; (g) Kozani 1995, best-fit model is ETAS; (h) Zakynthos 1997, best-fit model is ETAS.

4.4. The Aegean earthquake seismic sequence, 18 January 1982; $M_w = 7.0$

The location of this event is at the central part of the western branch of the North Aegean Trough (Fig. 1). The focal mechanism and spatial extend of the aftershock zone (Fig. 2d) indicate northeast striking dextral strike-slip faulting (Taymaz et al., 1991; Kiratzi et al., 1991). We delineated a study area by the vertices 39.0°N, 23.85°E; 40.05°N, 25.8°E; 40.9°N, 25.25°E; 39.8°N, 23.3°E, in which 158 aftershocks have occurred in a period of one year with a cut-off magnitude $M_0 = 3.7$, above which the data were assessed to be complete (Fig. 2d).

The smallest AIC was calculated for $M_{th} = 4.2$ (see Fig. 3d and Table 2) which identifies the best-fit model to be RETAS with the corresponding triggering magnitude. The pattern of grouping presumes the weakest events in the sample to be attached to aftershocks of $M_w = 4.2$ or larger. Data to model comparison (Fig. 7a–c) reveals a

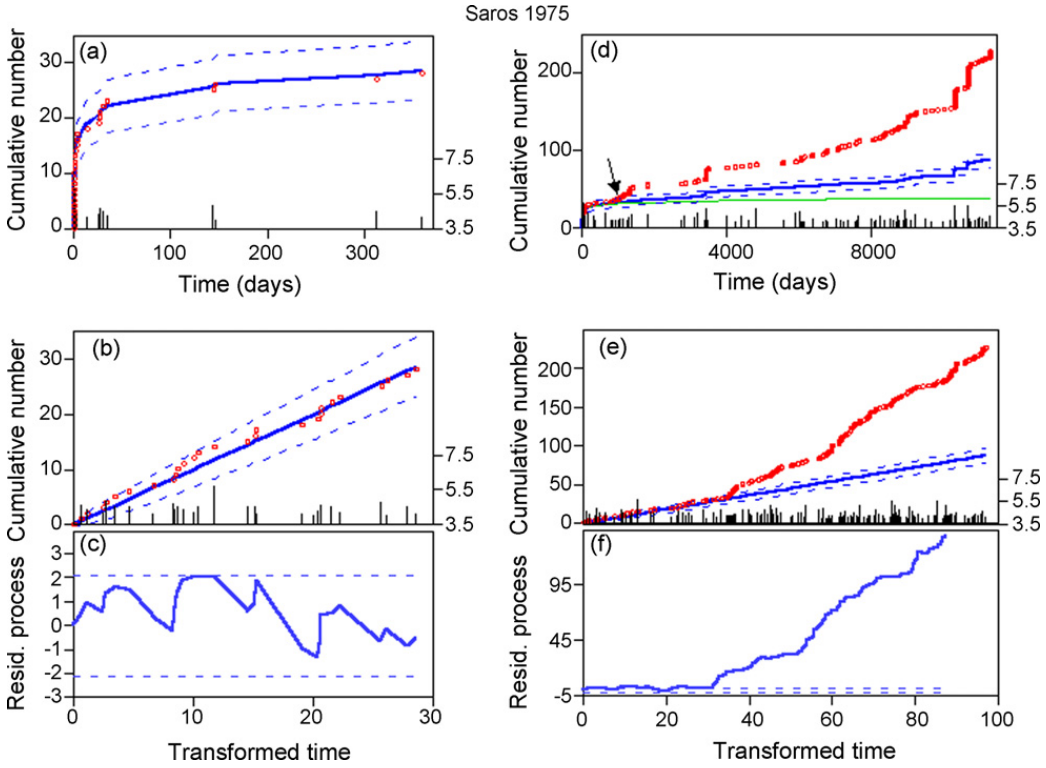

Fig. 4. Saros sequence, 1975; (a) Cumulative number of events in real time for the examined catalog of $N = 29$ aftershocks; blue continuous line – after the best-fit model, dashed lines – error bounds after the standard deviation, red circles – real cumulative number; (b) – the same for a transformed time axis (see in text); (c) – residual process (difference between real and model cumulative numbers and standard deviation of the residual process as error bounds). (d–f) The same as in '(a–c)' correspondingly but for earthquakes up to 2006 for the same zone (green continuous line – after the MOF model); Right vertical axes stand for aftershocks' magnitudes, plotted as vertical lines. (For interpretation of the references to colour in this figure legend, the reader is referred to the web version of the article.)

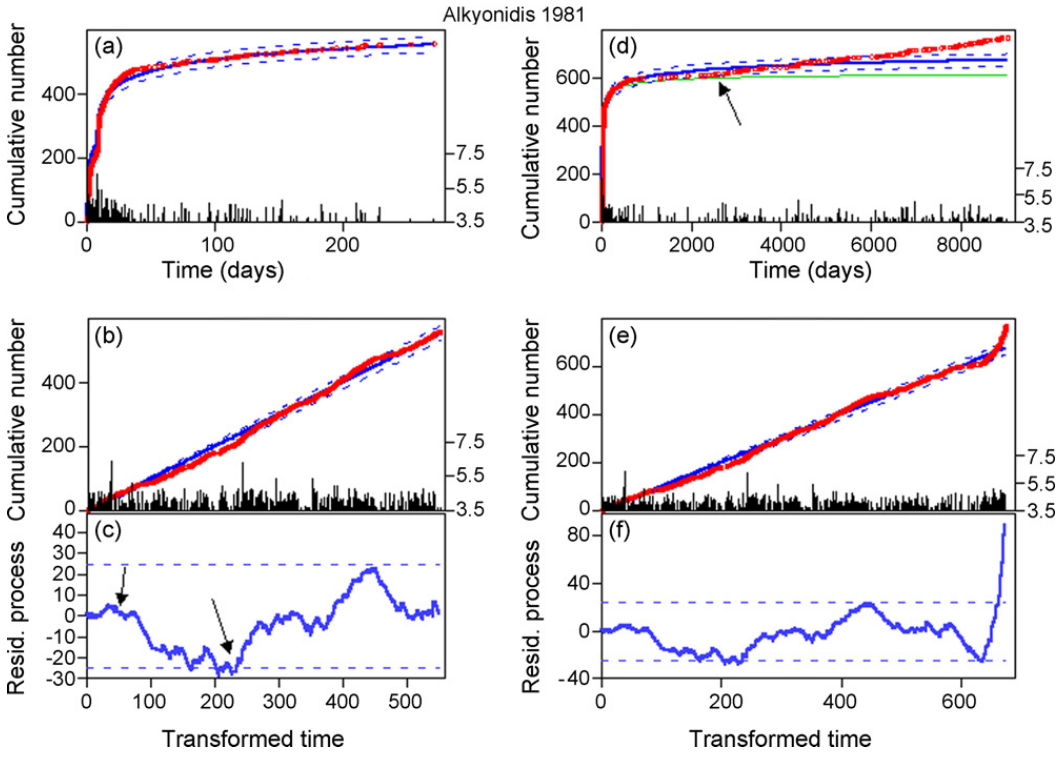

Fig. 5. Alkyonides sequence, 1981, $N = 553$—notation as in Fig. 4. (For interpretation of the references to colour in this figure legend, the reader is referred to the web version of the article.)

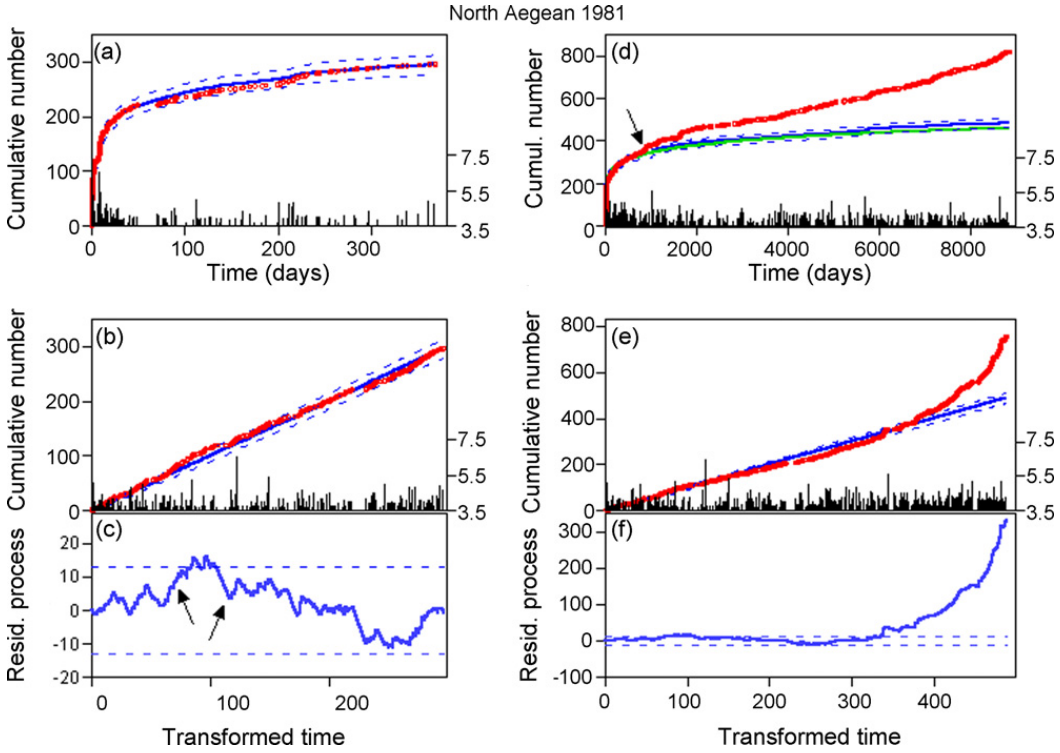

Fig. 6. North Aegean sequence, 1981, $N = 297$—notation as in Fig. 4. (For interpretation of the references to colour in this figure legend, the reader is referred to the web version of the article.)

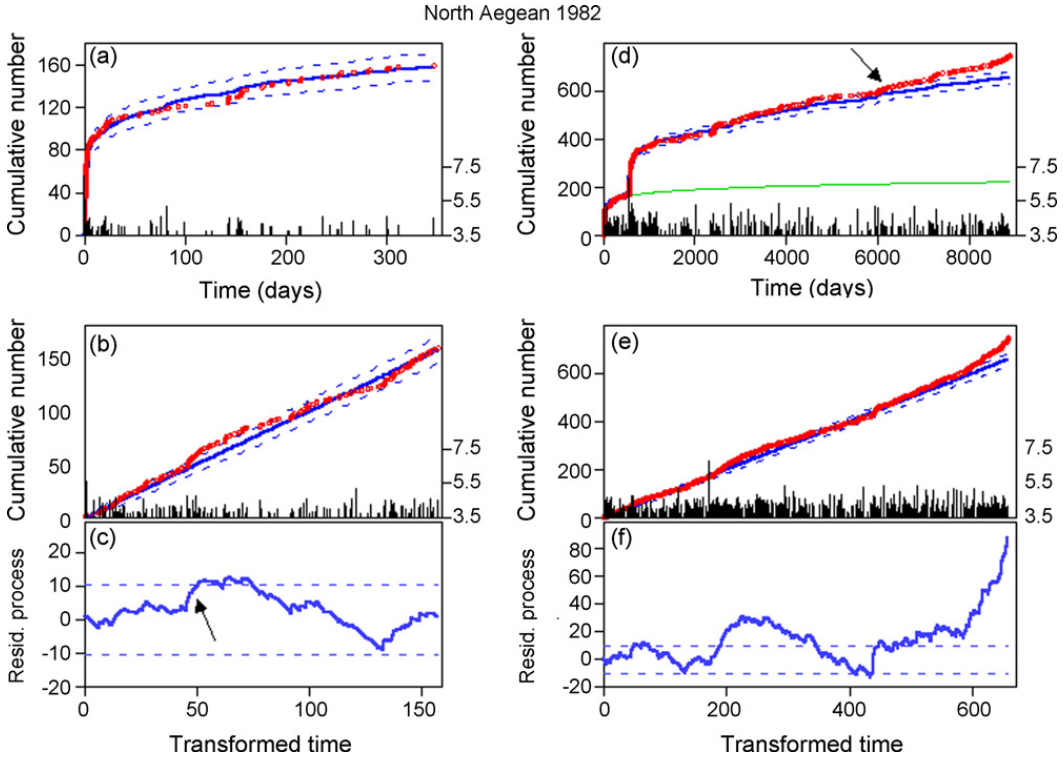

Fig. 7. North Aegean sequence, 1982, $N = 158$—notation as in Fig. 4. (For interpretation of the references to colour in this figure legend, the reader is referred to the web version of the article.)

relative rate increase at the end of the first day caused by a cluster of four shocks in the 4.5–4.8 magnitude range (follow arrow in Fig. 7c). After several days, this increase converts to a relative decrease lasting until the 130th day after the main event. This decrease is not related to any particular event and it is outstanding that the occurrence of the strongest aftershock of $M_w = 5.2$ does not cause rate change at all.

Examining Fig. 7d one can see a remarkably good correspondence between real seismicity (red circles) and the model curve (blue solid line). The RETAS model provides a very good forecast of the seismic process including the sequence of the $M_w = 6.8$ earthquake, which occurred in the region about a year and a half later. The real cumulative number follows the model more than 15 years after the 1982 main shock when real data diverges from the model curve (see arrow in Fig. 7d). Of course, in this prediction we use real (true) magnitudes (magnitudes are not simulated) but still an amazing fit between data and model is observed, considering that model parameters are estimated only from data covering the first year after the main shock occurrence. The duration of the aftershock sequence cannot be determined by comparing the data to the MOF model (green line) as the relaxation process is unambiguously not over when the next strong event in the region strikes in 1983.

4.5. Kefalonia seismic sequence, 17 January 1983; $M_w = 7.0$

The main shock is associated with the Cephalonia Transform Fault (Scordilis et al., 1985) in the area of central Ionian Islands (Fig. 1). Its fault plane solution and the ones of its largest aftershocks show right-lateral, strike-slip faulting with a thrust component, on a fault striking in an about NE–SW direction. The magnitude of completeness for this sequence was assessed to be $M_0 = 4.2$ and a number of $N = 364$ events were found to fulfill this requirement. They are confined inside a polygon defined by the vertices 37.5°N, 20.0°E; 38.0°N, 21.0°E; 38.5°N, 21.0°E; 39.0°N, 20.75°E; 38.25°N, 19.5°E (Fig. 2e) and cover the period till the end of 1983.

The model that provides the most appropriate picture of the aftershock process is the ETAS (Fig. 3e and Table 2). We can define a relative period of activation in Fig. 8b, c starting one day before the strongest aftershock of $M_w = 6.2$ (see arrow in Fig. 8c) and lasting about 3 days.

The sequence obviously is a complex one and the MOF model is inappropriate to distinguish the temporal details The MOF model is not suitable to determine aftershock duration, neither, as can be seen on Fig. 8d (green line). It is of importance to emphasize the exceptional good forecast of the real seismicity after the aftershock sequence which the ETAS model provides—a model developed on data of only 1 year 'predicts' well real seismicity behavior for more than 20 years (Fig. 8d). The real cumulative curve moves within the predicted error bounds for more than 20 years after the main shock and that remains so until the end of the period that our data cover (March 2006).

4.6. North Aegean seismic sequence, 6 August 1983; $M_w = 6.8$

The main shock of this sequence took place in a neighboring fault segment of the one associated with the 1982 occurrence, along the North Aegean Trough (Fig. 1). The spatial and temporal (a year and a half after) differentiation was the reason that this one was considered as a separate sequence. The northeast elongation of the aftershock zone (Fig. 2f) and the dextral strike-slip focal mechanism are similar to the 1982 earthquake (Taymaz et al., 1991; Kiratzi et al., 1991). The aftershocks which are stronger than the determined magnitude of completeness, $M_0 = 3.8$, are compiled for a period of 1 year after the main event in an area confined by the points 39.0°N, 23.85°E; 40.05°N, 25.8°E; 40.9°N, 25.25°E; 39.8°N, 23.3°E.

For this sequence, the triggering pattern seems to be different from the previous ones. The smallest AIC value (Fig. 3f) coincides with the magnitude cut-off $M_0 = M_{th} = 3.8$ and the finest data description is provided by the ETAS model, according to which even the weakest aftershock can trigger clusters. No significant departures of the model from the data are distinguished; the latter staying in the model curve error bounds for the entire period (Fig. 9a and b) and the residual process has a small standard deviation (Fig. 9c).

We examined carefully again both curves—model and real data in Fig. 9d, which represent the cumulative numbers after the 1-year period of analysis. The ETAS model fits the data in a period of about 1800 days and after that, the data deviates exceeding the model significantly. It is difficult to define the sequence duration as the data curve diverges from the MOF model gradually but we spot the aftershock activity to be over 800–1000 days after the start of the sequence (see arrow on Fig. 9d).

4.7. Kozani–Grevena seismic sequence, 13 May 1995; $M_w = 6.6$

The Kozani–Grevena earthquake of $M_w = 6.6$ occurred on 13 May 1995 in the central part of northern

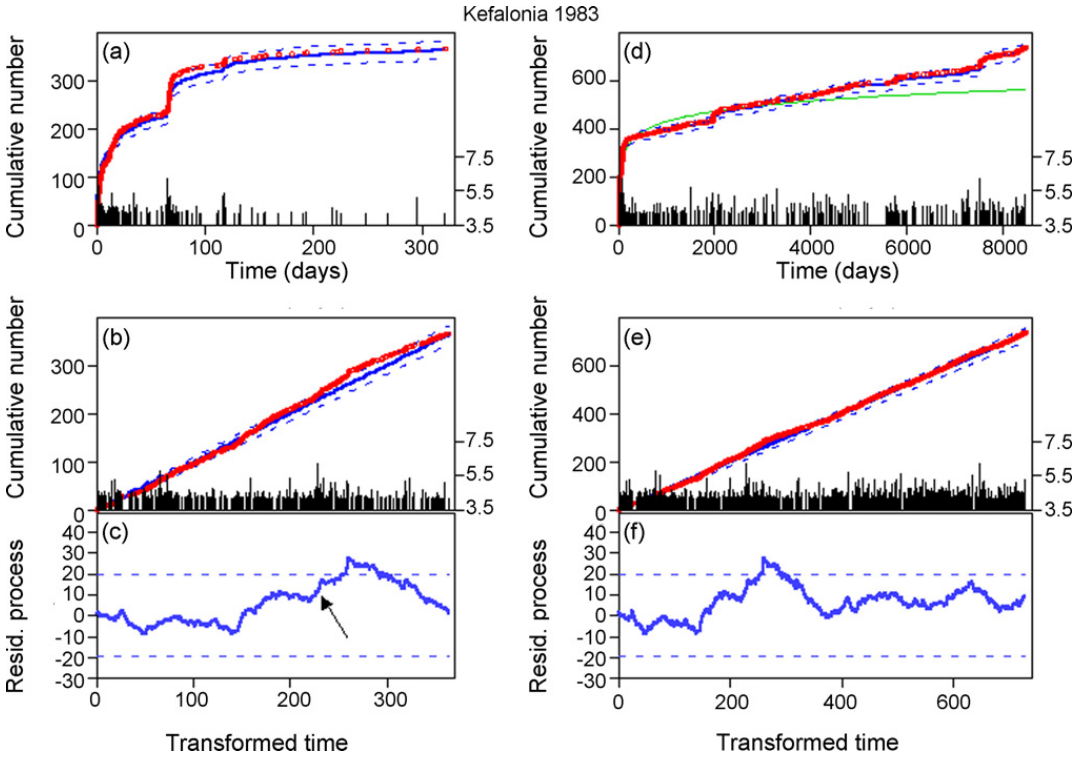

Fig. 8. Kefalonia sequence, 1983, $N = 364$—notation as in Fig. 4. (For interpretation of the references to colour in this figure legend, the reader is referred to the web version of the article.)

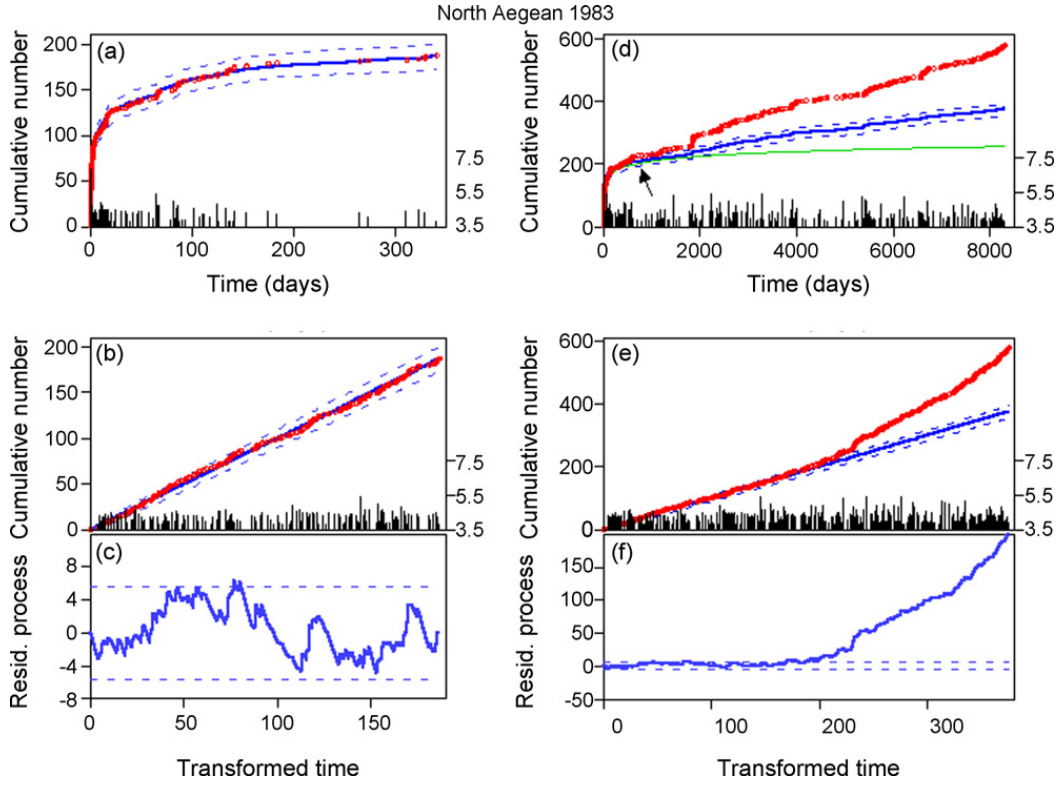

Fig. 9. North Aegean sequence, 1983, $N = 187$—notation as in Fig. 4. (For interpretation of the references to colour in this figure legend, the reader is referred to the web version of the article.)

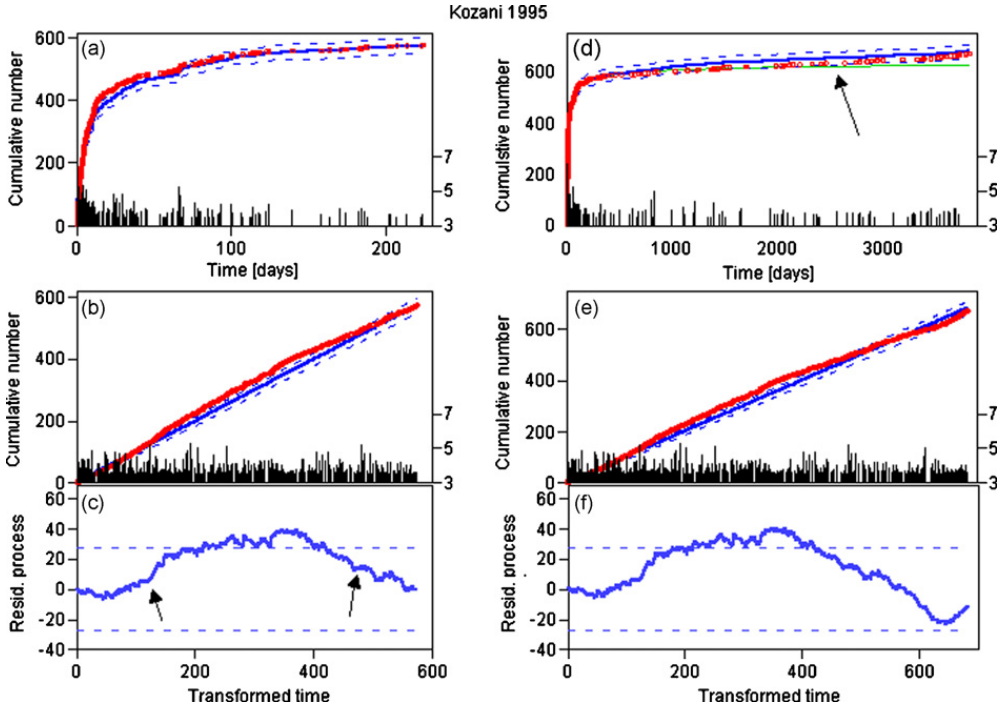

Fig. 10. Kozani sequence, 1995, $N = 573$—notation as in Fig. 4. (For interpretation of the references to colour in this figure legend, the reader is referred to the web version of the article.)

Greece (Fig. 1) and is associated with an ENE–WSW striking, north dipping normal fault. The first event was followed by a very high aftershock activity most of which was recorded after the deployment of a portable seismological network in the epicentral area (Hatzfeld et al., 1997). Although it occurred in a relatively low deformation area, the seismic sequence was intense and felt aftershocks continued to occur for several months after the mainshock occurrence (Papazachos et al., 1998b). For our analysis we prepared a catalog of 573 aftershocks up to the end of 1995, with magnitudes above the determined cut-off $M_0 = 3.5$ in a region defined by the points 39.8°N, 21.2°E; 39.8°N, 22.1°E; 40.4°N, 22.1°E; 40.4°N, 21.2°E (Fig. 2g).

The smallest AIC value in Fig. 3g is for a triggering magnitude of $M_{th} = 3.5$, which is equal to the magnitude cut-off and this result recognizes the ETAS model to fit best the temporal evolution of the seismic sequence. Both model and real cumulative curves are illustrated in Fig. 10a and b. In Fig. 10c one can observe a relative activation commencing at the end of the second day after an $M_w = 5.2$ shock (see arrows). It lasts about 15 days and turns to a rate decrease which keeps on until the occurrence of a second aftershock of the same magnitude, subsequent to which model and data progress quite closely (see bottom part of Fig. 10a). The periods of relative discrepancies do not seem to mark any particular event.

In Fig. 10d, the MOF model (green line) starts to depart from real data (red circles) at approximately 2000–2300 days after the main shock (see arrow), which is an estimate of the aftershock sequence duration. This is a highly rough assessment, however, as the seismicity in the region after the sequence is very low, and, therefore, this impedes a more precise evaluation. After the end of 1995 where the studied period ends, the ETAS model persists to depict well the real seismicity, starting to exceed it after an earthquake of $M_w = 5.0$ which caused no aftershock activity at all. Overall, the best-fit model provides a very good forecast of seismicity subsequent to the aftershock sequence till the end of October 2005.

4.8. Zakynthos seismic sequence, 18 November 1997; $M_w = 6.6$

The main shock took place at the northwestern part of the Hellenic Arc (Fig. 1) associated with thrusting on the subduction interface. It occurred on November 18 and was followed by a strong aftershock of $M_w = 6.0$ just six minutes later, the epicenter of the latter being to the west of the main shock. We compiled a catalog of $N = 640$ events in a one year period with a magnitude cut-off $M_w = 3.8$ which was determined with the help of the ZMAP software (Wiemer, 2001). The epicenters are confined in between the points 36.9°N, 19.8°E; 36.9°N, 21.4°E; 38.3°N, 21.4°E; 38.3°N, 19.8°E (Fig. 2h).

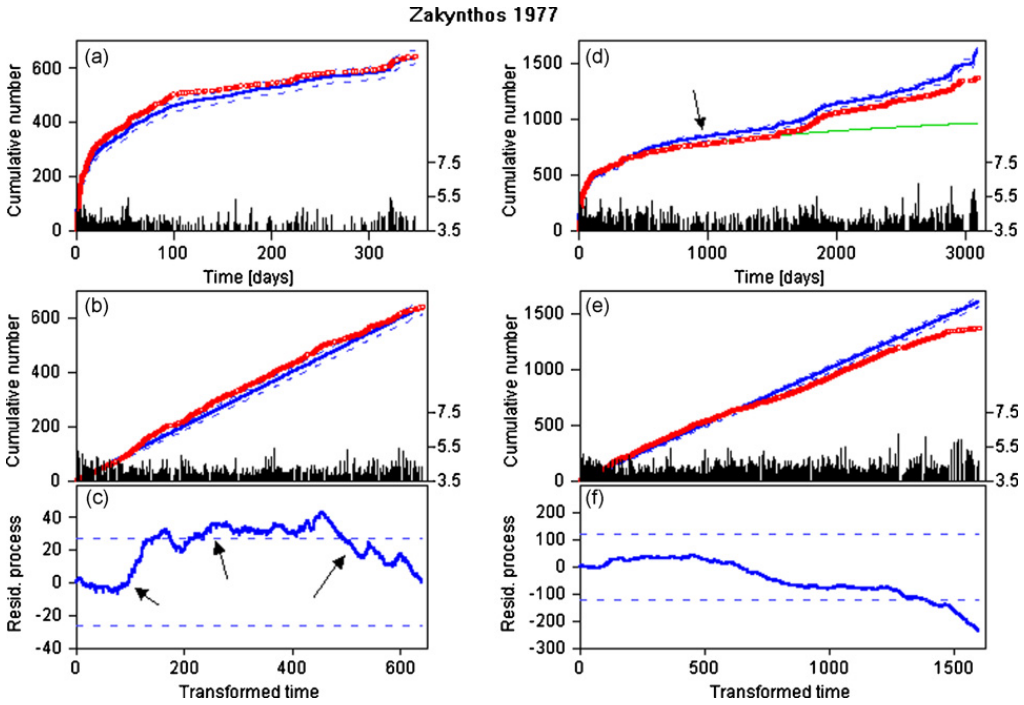

Fig. 11. Zakynthos sequence, 1997, $N = 640$—notation as in Fig. 4. (For interpretation of the references to colour in this figure legend, the reader is referred to the web version of the article.)

The results from the stochastic modeling are presented on Fig. 3h where the smallest AIC value recognizes the model giving the finest data description to be the one for which $M_w = M_0 = 3.8$ (RETAS coinciding with ETAS). The data curves in Fig. 11a, b, c expose an intensive comparative activation from the 5th to the 20th day, after which they follow the model curves slope, but real data exceeds the error bounds for quite a long period lasting more than 150 days (follow arrows in Fig. 11c from left to right). From about the 100th to the 165th day a relative rate decrease is seen subsequently to which data and model move close to each other. None of the above discrepancies are related to any particular strong aftershock but the peculiarity here concerns the large number of aftershocks with magnitudes $M_w \geq 4.5$, which could be the reason for the observed temporal behavior.

In Fig. 11d, we detect that the MOF model (green line) deviates from real data (red circles) about 1600–1700 days after the beginning of the sequence. We assume this an evaluation of the aftershock process duration. This result departs substantially from the average duration values for Greece obtained by Kourouzidis et al. (2004) as were the cases with the Alkyonides and the Kozani sequences, although the background seismicity here is not low. The seismic process forecast produced by the best-fit ETAS model after the conclusion of the examined sample is not very good as data and model start to diverge even before the end of the aftershock sequence (after the 1000th–1100th day; see arrow on Fig. 11d). On the other hand, this departure progresses very slowly and both curves are very similar in form which reveals that the model still captures a lot of the real process temporal features.

5. Features of the RETAS model simulation

A purpose of high priority in the stochastic modeling of seismicity is the possibility to make shorter or longer forecasts of the real process. We have found, that for several (four cases out of eight) aftershock sequences the recognized best-fit model portrays very well the data curve after the end of the relaxation process although model parameters were estimated on aftershock data only. These results seem very interesting and promising as they hint that we have perhaps identified some general features of seismic interaction and triggering in these regions. We have to keep in mind, however, that this is not a real prediction of the process as we input in the model real magnitudes of which we do not have preliminary knowledge. In fact, if we intend to avoid this problem we have to forecast magnitudes, too, that is, we must simulate the model. The simulation procedure of the RETAS model is presented by Gospodinov and Rotondi (2006) in a greater detail and here we generated a set of aftershock

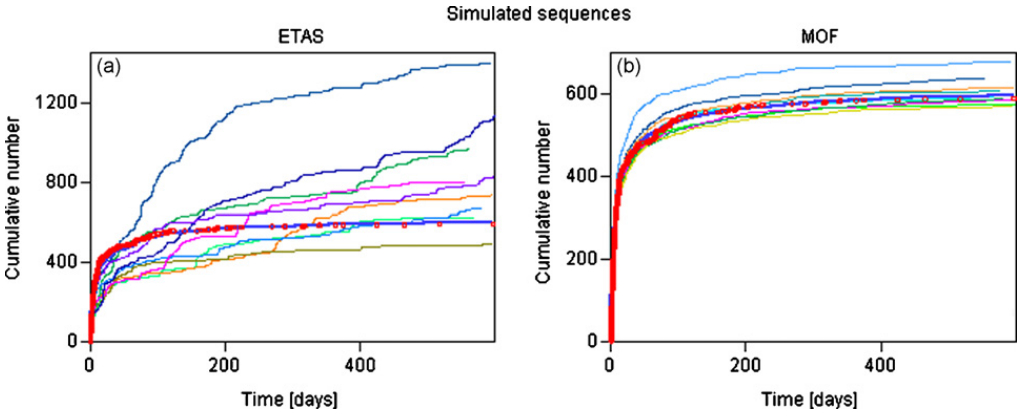

Fig. 12. Simulated sequences; (a) Sequences simulated after the best-fit ETAS model with parameter values after the Kozani aftershock sequence (see Table 2); Solid blue line is the ETAS model curve for the Kozani sequence and red circles stand for the real cumulative number; the thinner curves of different colors depict simulations of the ETAS model, generated after a procedure offered by Gospodinov and Rotondi (2006); (b) Notation as in 'a' but for the MOF model for the Kozani aftershock sequence. (For interpretation of the references to colour in this figure legend, the reader is referred to the web version of the article.)

sequences to analyze some problems accompanying this topic.

In practical terms to predict the aftershock process in a region with the help of the RETAS model means to be able to calculate future activity immediately after the main shock using formulae (3) and (6). Assuming that the model parameter values are known in advance, the future aftershocks' magnitudes were generated randomly after the recurrence law of the real events. Bearing it in mind, we produced a set of random sequences following the best-fit ETAS model identified for the Kozani aftershock process (parameter values in Table 2). The cumulative curves of these series are plotted in Fig. 12a, while in Fig. 12b a similar set created after the MOF model for the same aftershock sequence is illustrated.

It is impressing to observe how poorly the simulated data after the ETAS model tracks the real one, a result found also in previous investigations (Helmstetter et al., 2003). The generated curves diverge largely and very quickly, even from the first days. Furthermore, their pattern is quite different from the real curve. As the only actual event in the simulation procedure is the main shock with its magnitude, the created data do reveal some decreasing behavior but at a much lesser extent than the genuine aftershock process and for a short period. After that, for a lot of the simulated sequences the rate starts fluctuating around a constant value. In fact, these results are not so astonishing as the model itself presented by formula (3) does not foresee a decaying behavior. In that aspect, the more interesting question is how such a stochastic process makes a very good fit of the real data (thicker blue line in Fig. 12a). The answer is in the magnitudes—that of the main event and the ones of the real aftershocks. We assume in the model that aftershock magnitudes are independent from each other and from their times of occurrence, which now turns not to be completely correct. In our opinion, the observed divergence of the simulated curves can be explained if we assume that for the real data the magnitudes of the aftershocks tend to be larger at the beginning of the sequence—a feature that is not considered in the stochastic model and in the simulation procedure.

The MOF model simulations in Fig. 12b provide much better long-term forecasts of the aftershock temporal performance. In fact the results up to now disclose that the ETAS model makes a good retrospective description of an aftershock sequence, while for real-time prediction it can be used for a short-term period only which depends on the rate of the process at the moment. It is the modified Omori formula, which can provide a long-term picture of the future aftershock process on the average although missing some of the process details.

6. Discussion and conclusions

We analyzed the temporal decay of eight aftershock sequences in the area of Greece after 1975 with main shocks magnitudes of $M_w \geq 6.6$. We applied the RETAS stochastic model, which allows choosing the best-fit model for each data set thus enabling the possibility to recognize the prevailing clustering pattern of the relaxation process in the examined areas. In four of the cases, triggering potential seems to have aftershocks above a certain magnitude threshold (RETAS model) and they are expected to induce secondary activity. For the other four sequences, the analysis selected the ETAS model to offer the most appropriate depiction of the aftershock temporal distribution, which presumes that all shocks to

the smallest ones in the sample can cause consequential aftershocks. Actually, the versions of the RETAS model corresponding to the triggering magnitude values introduce a measure of the secondary activity in a sequence. For a sequence following the MOF model no secondary clustering is expected while for another one after the ETAS model subclustering is to be found for all events down to the weakest ones (Kefalonia, 1983; North Aegean, 1983; Kozani, 1995; Zakynthos, 1997). The sequences that fit the intermediate versions of the RETAS model expose a temporal pattern characterized by secondary aftershock activity only for events above a certain magnitude. Similar cases are the Alkyonides 1981 sequence, where only the three strongest events in the group control the type of clustering, as well as the sequences in Saros 1975, North Aegean 1981, and North Aegean 1982.

Selecting a best-fit RETAS model for each sequence permits the recognition of some relative to model activations or rate decrease. For several of them they seem to be related to the strongest aftershocks in the sequence (Alkyonides, 1981; North Aegean, 1981; North Aegean, 1983) while in other cases they are not entitled to any particular event (Kozani, 1995; Zakynthos, 1997). It was a matter of key importance in the present study to verify probable relations between selected stochastic models and any aspects of the geotectonic structure or physical processes underlying seismicity. Attempts to explain aftershock temporal decay are usually associated with phenomena like static fatigue, visco-elastic relaxation or diffusion (fluids), but in the lack of an exact theory any effort to correlate these processes to stochasticity would turn to be speculative. Thus, we are tempted to consider an idea according to which the relaxation pattern after the main event is controlled by optimally oriented Coulomb stress changes. Depending on the tectonic structure of the region, these changes will or will not trigger secondary aftershocks thus defining the activity to follow different versions of the RETAS model.

Another result of our analysis which could indirectly support feasible connection between stochastic modeling and region's tectonic characteristics is the fact that for four out of eight cases we obtained promising forecasts of seismicity after the aftershock sequence on models based only on aftershock data. These predictions, however, were formulated by exploiting real magnitudes and when we apply simulated magnitudes, the forecast is much worse. It becomes evident that the ETAS model cannot provide an appropriate simulation of real seismicity as it assumes random magnitude values in the simulation procedure and in real sequences stronger aftershocks often have a bigger probability of occurrence at the beginning of the process.

We would also like to draw reader's attention on the fact that for all eight sequences the minimum AIC values are calculated for models with background seismicity $\mu = 0$ which reveals that such models better depict aftershock temporal behavior. In Table 2 we also present model parameters for $\mu <> 0$ for comparison, but it must be noted that these model versions are not appropriate to forecast seismic activity after the sequence is over, as the parameter μ seems to be overestimated on the aftershock data. These results provoke the question of whether we should include the background seismicity μ in the stochastic modeling of an aftershock sequence, when seismicity is mainly controlled by the stress field changes after the main shock.

We attempted to estimate the duration of the relaxation process assuming that the end of each sequence is marked by the divergence of real seismicity from the MOF model, the latter known to represent pure aftershock activity. No dependence between aftershock duration and main shock's magnitude was found but the period of activity for some of the sequences was evaluated to be quite longer than the average values for the region. A probable dependence between aftershock duration and background seismicity rate could be the explanation of these results as generally longer activity periods were obtained for regions of lower seismicity. The obtained results give a hint that low rate of stress build-up could be related to longer duration of the relaxation process in a region.

Acknowledgements

The GMT system (Wessel and Smith, 1998) was used to plot some of the figures. The creative comments of two anonymous reviewers and the editorial assistance of Prof. Keke Zhang are greatly appreciated. This study was supported by the bilateral research project between Greece and Bulgaria EPAN-M.4.3.6.1 and BG-9/05. Geophysics Department contribution 700.

References

Akaike, H., 1974. A new look at the statistical model identification. IEEE Trans. Automat. Contr. AC 19, 716–723.

Bath, M., 1965. Lateral inhomogeneities in the upper mantle. Tectonophysics 2, 488–514.

Bath, M., 1973. Introduction to Seismology. Birkhauser, Basel, 1973.

Console, R., Murru, M., 2001. A simple and testable model for earthquake clustering. J. Geophys. Res. 106, 8699–8711.

Console, R., Murru, M., Lombardi, A.M., 2003. Refining earthquake clustering models. J. Geophys. Res. 108, 2468, doi:10.1029/2002JB002130.

Drakatos, G., 2000. Relative seismic quiescence before large aftershocks. Pure Appl. Geophys. 157, 1407–1421.

Drakatos, G., Latoussakis, J., 1996. Some features of aftershock patterns in Greece. Geophys. J. Int. 126, 123–134.

Gospodinov, D., Rotondi, R., 2006. Statistical analysis of triggered seismicity in the Kresna Region of SW Bulgaria (1904) and the Umbria-Marche Region of Central Italy (1997). Pure Appl. Geophys. 163, 1597–1615.

Guo, Z., Ogata, Y., 1997. Statistical relations between the parameters of aftershocks in time, space and magnitude. J. Geophys. Res. 102, 2857–2873.

Hatzfeld, D., Karakostas, V., Ziazia, M., Selvaggi, G., Leborgne, S., Berge, C., Guiguet, R., Paul, A., Voidomatis, P., Diagnourtas, D., Kassaras, I., Koutsikos, I., Makropoulos, K., Azzara, R., Di Bona, M., Baccheschi, S., Bernard, P., Papaioannou, C., 1997. The Kozani–Grevena (Greece) earthquake of 13 May 1995 revisited from a detailed seismological study. Bull. Seismol. Soc. Am. 87, 463–473.

Helmstetter, A., Sornette, D., Grasso, J.-R., 2003. Mainshocks are aftershocks of conditional foreshocks: how do foreshock statistical properties emerge from aftershock laws. J. Geophys. Res. 108, 2046, doi:10.1029/2002JB001991.

International Seismological Center, 2006. On-line Bulletin, http://www.isc.ac.uk/Bull. International Seismological Center, Thatcham, United Kingdom.

Kagan, Y.Y., 1991. Likelihood analysis of earthquake catalogues. J. Geophys. Res. 106, 135–148.

Kiratzi, A., Wagner, G., Langston, C., 1991. Source parameters of some large earthquakes in northern Aegean determined by body waveform inversion. Pure Appl. Geophys. 135, 515–527.

Kisslinger, C., Jones, L.M., 1991. Properties of aftershocks in southern California. J. Geophys. Res. 96, 11947–11958.

Kourouzidis, M., Karakaisis, G., Papazachos, B., Makropoulos, C., 2004. Properties of foreshocks and aftershocks in the area of Greece. Bull. Geol. Soc. Greece XXXVI, 1422–1431.

Latoussakis, J., Stavrakakis, G., Drakopoulos, J., Papanastassiou, D., Drakatos, G., 1991. Temporal characteristics of some earthquake sequences in Greece. Tectonophysics 193, 299–310.

Louvari, E., 2000. A detailed seismotectonic study of the Aegean and neighboring regions based on focal mechanisms of moderate sized earthquakes. Ph.D. Thesis. Aristotle Univ. Thes., Thessaloniki, p. 309.

McKenzie, D.P., 1970. The plate tectonics of the Mediterranean region. Nature 226, 239–243.

McKenzie, D.P., 1972. Active tectonics of the Mediterranean region. Geophys. J. R. Astron. Soc. 30, 109–185.

McKenzie, D.P., 1978. Active tectonics of the Alpine–Himalayan belt: the Aegean Sea and surrounding regions. Geophys. J. R. Astron. Soc. 55, 217–254.

Matsu'ura, R., 1986. Precursory quiescence and recovery of aftershock activity before some large aftershocks. Bull. Earthq. Res. Inst. Univ. Tokyo 16, 1–65.

Musmeci, F., Vere-Jones, D., 1992. A space–time clustering model for historical earthquakes. Ann. Inst. Stat. Math. 44, 1–11.

Ogata, Y., 1988. Statistical models for earthquake occurrences and residual analysis for point processes. J. Am. Stat. Assoc. 83, 9–27.

Ogata, Y., 1989. Statistical model for standard seismicity and detection of anomalies by residual analysis. Tectonophysics 169, 159–174.

Ogata, Y., 1992. Detection of precursory relative quiescence before great earthquakes through a statistical model. J. Geophys. Res. 97, 19845–19871.

Ogata, Y., 1993. Space–time modeling of earthquake occurrences. Bull. Int. Stat. Inst. 55 (Book 2), 249–250.

Ogata, Y., 1998. Space–time point-process models for earthquake occurrences. Ann. Inst. Stat. Math. 50, 379–402.

Ogata, Y., 2001. Exploratory analysis of earthquake clusters by likelihood-based trigger models. J. Appl. Prob. 38A, 202–212.

Ogata, Y., 2005a. Detection of anomalous seismicity as a stress change sensor. J. Geophys. Res. 110, B05306, doi:10.1029/2004JB003245.

Ogata, Y., 2005b. Synchronous seismicity changes in and around the northern Japan preceding the 2003 Tokachi-oki earthquake of M8.0. J. Geophys. Res. 110, B08305, doi:10.1029/2004JB003323.

Ogata, Y., Jones, L.M., Toda, S., 2003. When and where the aftershock activity was depressed: contrasting decay patterns of the proximate large earthquakes in southern California. J. Geophys. Res. 108, 2318, doi:10.1029/2002JB002009.

Omori, F., 1894. On the aftershocks of earthquakes. J. Colloid Sci. Imp. Univ. Tokyo 7, 111–200.

Papadimitriou, E.E., 1993. Focal mechanism along the convex side of the Hellenic arc. Bull. Geof. Teor. Appl. 35, 401–426.

Papazachos, B.C., Comninakis, P.E., 1970. Geophysical features of the Greek island arc and eastern Mediterranean ridge. In: Com. Ren. Des Sceances de la Conference Reunie a Madrid, 1969, vol. 16, pp. 74–75.

Papazachos, B.C., Comninakis, P.E., 1971. Geophysical and tectonic features of the Aegean arc. J. Geophys. Res. 76, 8517–8533.

Papazachos, B.C., Comninakis, P.E., Papadimitriou, E.E., Scordilis, E.M., 1984. Properties of the February–March 1981 seismic sequence in the Alkyonides gulf of Central Greece. Ann. Geophys. 25, 537–544.

Papazachos, B.C., Kiratzi, A.A., Karakostas, B.G., 1997. Toward a homogeneous moment magnitude determination in Greece and surrounding area. Bull. Seismol. Soc. Am. 87, 474–483.

Papazachos, B.C., Papadimitriou, E.E., Kiratzi, A.A., Papazachos, C.B., Louvari, E.K., 1998a. Fault plane solutions in the Aegean Sea and the surrounding area and their tectonic implications. Bull. Geof. Teor. Appl. 39, 199–218.

Papazachos, B.C., Karakostas, B.G., Kiratzi, A.A., Papadimitriou, E.E., Papazachos, C.B., 1998b. A model for the 1995 Kozani–Grevena seismic sequence. J. Geodyn. 26, 217–231.

Papazachos, B.C., Comninakis, P.E., Karakaisis, G.F., Karakostas, B.G., Papaioannou, Ch.A., Papazachos, C.B., Scordilis, E.M., 2006. A Catalogue of Earthquakes in Greece and Surrounding Area for the Period 550BC–2005. Geophysics Laboratory, University of Thessaloniki.

Papazachos, C.B., Kiratzi, A.A., 1996. A detailed study of the active crustal deformation in the Aegean and surrounding area. Tectonophysics 253, 129–153.

Rathbun, S.L., 1993. Modeling marked spatio-temporal point patterns. Bull. Int. Stat. Inst. 55 (Book 2), 379–396.

Rathbun, S.L., 1994. Asymptotic properties of the maximum likelihood estimator for spatio-temporal point processes. Spatial Stat. J. Stat. Plann. Inform. 51, 55–74 (Special issue).

Reasenberg, P.A., Jones, L.M., 1994. Earthquake aftershocks: update. Science 265, 1251–1252.

Schoenberg, R.P., 1997. Assessment of multi-dimensional point processes. Ph.D. Thesis. University of California, Berkeley.

Scordilis, E.M., Karakaisis, G.F., Karakostas, B.G., Panagiotopoulos, D.G., Comninakis, P.E., Papazachos, B.C., 1985. Evidence for transform faulting in the Ionian Sea: the Cephalonia Island earthquake sequence. Pure Appl. Geophys. 123, 388–397.

Taymaz, T., Jackson, J., McKenzie, D., 1991. Active tectonics of the north and central Aegean Sea. Geophys. J. Int. 106, 433–490.

Utsu, T., Seki, A., 1955. Relation between the area of aftershock region and the energy of the main shock (in Japanese). Zisin 2nd Ser. 7, 233–240.

Utsu, T., 1970. Aftershocks and earthquake statistics (II): further investigation of aftershocks and other earthquake sequences based on a new classification of earthquake sequences. J. Fac. Sci., Hokkaido Univ., Ser. VII (Geophys.) 3, 198–266.

Utsu, T., Ogata, Y., Matsu'ura, R.S., 1995. The centenary of the Omori formula for a decay law of aftershock activity. J. Phys. Earth 43, 1–33.

Vere-Jones, D., 1970. Stochastic models for earthquake occurrence (with discussion). J. R. Stat. Soc. Ser. B 32, 1–62.

Vere-Jones, D., 1992. Statistical methods for the description and display of earthquake catalogues. In: Walden, A., Guttorp, P. (Eds.), Statistics in the Environmental and Earth Sciences. Edward Arnold, London, pp. 220–236.

Vere-Jones, D., Davies, R.B., 1966. A statistical survey of earthquakes in the main seismic region of New Zealand. Part 2. Time series analyses. N. Z. J. Geol. Geophys. 9, 251–284.

Wessel, P., Smith, W.H.F., 1998. New, improved version of the generic mapping tools released. EOS Trans. AGU 79, 579.

Wiemer, S., 2001. A software package to analyze seismicity: ZMAP. Seism. Res. Lett. 72, 373–382.

Zhao, Z., Matsumara, K., Oike, K., 1989. Precursory change of aftershock activity before large aftershock: a case study for recent earthquakes in China. J. Phys. Earth 37, 155–177.

Zhuang, J., Ogata, Y., Vere-Jones, D., 2002. Stochastic declustering of space–time earthquake occurrences. J. Am. Stat. Assoc. 97, 369–380.